2024 IEEE/RSJ International Conference on Intelligent Robots and Systems (IROS)
October 14-18, 2024. Abu Dhabi, UAE

Efficient Estimation of Frequency Response Functions of Industrial Robots Using the Local Rational Method

Stefanie A. Zimmermann[1], Stig Moberg[2]

Abstract— **Nonparametric estimates of frequency response functions (FRFs) are often suitable for describing the dynamics of a mechanical system. If treating these estimates as measurements, they can be used for parametric identification of, e.g., a gray-box model. This paper shows that a more accurate parametric model can be identified based on local parametric FRF estimates, giving a shorter total experiment time, compared to classical methods. Classical methods for nonparametric FRF estimation of MIMO (Multiple Input Multiple Output) systems require at least as many experiments as the system has inputs. Local parametric FRF estimation methods have been developed for avoiding multiple experiments. In this paper, these local methods are adapted and applied for estimating the FRFs of a 6-axes robotic manipulator, which is a nonlinear MIMO system operating in closed loop. The aim is to reduce the experiment time and amount of data needed for identification. The resulting FRFs are analyzed in an experimental study and compared to estimates obtained by classical MIMO techniques.**

I. Introduction and related work

Accurate models of robotic manipulators are needed for many purposes, and they are of particular importance for control design. Today, most control algorithms are based on parametric models, describing the dynamic behavior of the robot in all possible applications. Combining prior knowledge and a large amount of experimental data, high-fidelity models can be identified [1]. The aim of this work is to reduce the experiment time while keeping the model's quality. This will make the identification procedure faster, and will furthermore reduce wear during measuring.

This paper follows a frequency-domain approach for parameter identification of a nonlinear gray-box model. Linearizations of the system in different configurations are used, while requiring the identified model to be global w.r.t. configuration, pay- and armloads. Aiming to identify a parametric robot model, the first step is the estimation of the system's frequency response function (FRF). This is often done with classical nonparametric methods, which require at least as many experiments as the system has inputs. For improving the quality of the FRF estimate, additional experiments are done and averaging techniques applied. At the cost of many experiments, this method has shown to give accurate FRF estimates, assuming appropriate excitation signals [2].

In order to reduce the experiment time, this paper evaluates a class of potentially data-efficient methods, local parametric FRF estimation methods, and compare these to the classical nonparametric methods. The key idea of local parametric methods is to assume that the FRF is a smooth function of frequency and to locally approximate it by, e.g., a polynomial (Local Polynomial Method, LPM), or a rational function (Local Rational Method, LRM) in a narrow frequency band around a central frequency [3], [4], [5]. This method allows to estimate the MIMO-FRFs with only one experiment.

In [4], the theory is developed for linear dynamic multivariable output error problems. The method is used for nonlinear systems in [5] and it is generalized for noisy input-output data (errors-in-variables problem), as well as for closed loop identification. In order to reduce the Mean Square Error of the FRF estimates, constraints between the coefficients of the polynomials at neighboring frequencies are proposed in [6]. Recently, the local techniques have been revisited [7] and a new method combining LPM and LRM has been developed, including an automatic local model-order selection procedure. Besides the data efficiency, the choice of the multivariable rational model parametrizations is a key aspect of LRM. Different choices are discussed in [8].

In this paper, the LRM is applied for estimating the FRFs of a robotic manipulator, a nonlinear MIMO system operating in closed loop. To our knowledge, LRM has not yet been used to estimate the FRFs of a robot. Here, the final goal is to identify a physically parameterized robot model based on these FRFs, which is suitable for control purposes. LRM has been analyzed in the context of Spectral Analysis (e.g. [8]), while in this paper, two multivariable LRM parametrizations are experimentally compared with classical, purely nonparametric, averaging techniques that involve multiple experiments. Furthermore, we propose to combine multiple LRM estimates by logarithmic averaging for improving the estimate. The main contribution of this paper is an experimental study showing that LRM estimates, compared to classical nonparametric estimates,

- give lower parameter bias, i.e. higher accuracy, in gray-box identification,
- offer more time efficient gray-box identification.

In order to achieve these improvements the following choices were found to be essential when applying LRM:

- MIMO-parametrization of the local models,
- using the reference signal (Joint Input-Output approach),
- logarithmically averaging multiple LRM estimates.

Local parametric and classical nonparametric methods for FRF estimation are reviewed in Section III. Before, Section II introduces the parametric robot model to be identified and

[1]Department of Electrical Engineering, Linköping University, Sweden, stefanie.zimmermann@liu.se
[2]ABB Robotics, Västerås, Sweden, stig.moberg@se.abb.com

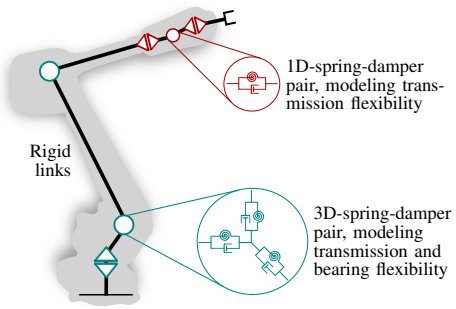

Fig. 1. Gray-box model structure of an 6-axes manipulator.

the method for parameter estimation. Results concerning the FRF estimation are presented in Section V, and results concerning the parametric robot identification are shown in Section VI. Section VII summarizes conclusions.

II. Parametric model identification

The final goal is to identify the stiffness parameters of the gray-box robot model presented in the following. The parameter estimation is based on nonparametric FRF estimates as outlined in Section II-B.

A. Gray-box model structure

The robot under consideration is a 6-axes serial-link manipulator. The model structure proposed in [9] is used, where a rigid body model with 6 degrees of freedom is extended by flexibility and friction in the joints. The transmission stiffness of joints 4 to 6 is modeled by linear spring-damper pairs, acting in the direction of rotation of the joint. Due to high loading, the transmission stiffness of joints 1 to 3 is described as nonlinear function, and two more linear spring-damper pairs are added for taking into account bearing and structural flexibility. Figure 1 shows a drawing of the robot model structure. The vector of joint angles on the arm side of the gearbox is $q_a \in \mathbb{R}^{6\times 1}$ and the angles on motor side are $q_m \in \mathbb{R}^{6\times 1}$. A realization of q_a is called *robot configuration*. The angular motion between the rigid bodies due to elastic effects that act perpendicular to the direction of transmission is described by the variables q_e. Here, we model these unactuated rotations q_e in two Cartesian directions only in the first three joints of the robot, thus the vector q_e has dimension 6. In order to derive a state-space model, we choose the state vector $x = [q_m, q_a, q_e, \dot{q}_m, \dot{q}_a, \dot{q}_e]^T$, the applied motor torque as input u, and the motor angular velocity $\dot{q}_m$ as output. We obtain the equations of motions:

$$\dot{x} = f(x,u,\theta) = \begin{bmatrix} \dot{q}_m \\ \dot{q}_a \\ \dot{q}_e \\ M_m^{-1}(u - \tau_{fm} - r_g\tau_g) \\ M_{ae}^{-1}\left(\begin{bmatrix}\tau_g(\theta)\\ \tau_e(\theta)\end{bmatrix} - c_{ae} - g_{ae}\right) \end{bmatrix} \quad (1)$$

$$y = h(x,u,\theta) = \dot{q}_m$$

where M_m is the matrix of motor inertias, $\tau_{fm}(\dot{q}_m)$ is the motor and gearbox friction (assumed to be located mainly on the input side of the gearbox), r_g is the matrix of inverse gear ratios, $M_{ae}(q_a, q_e)$ is the inertia matrix, $c_{ae}(q_a, q_e, \dot{q}_a, \dot{q}_e)$ is the velocity dependent torque, and $g_{ae}(q_a, q_e)$ is the gravity torque. The gear torque is

$$\tau_g(\theta) = \tau_k(k_g, \Delta q_a) + d_g\left(r_g\dot{q}_m - \dot{q}_a\right)$$
$$\tau_e(\theta) = -k_e q_e - d_e\dot{q}_e$$

where k_g, k_e, d_g and d_e are the joint stiffness and damping constants in the direction of transmission (index g) and perpendicular to it (index e). The transmission stiffness $\tau_k(k_g, \Delta q_a)$ is a nonlinear function dependent on the gear deflection $\Delta q_a = r_g q_m - q_a$. In the scope of this work, the rigid body parameters are assumed to be known, while a friction model is identified separately. The challenge of identification is therefore restricted to estimating the parameters of the nonlinear stiffness function τ_k and the parameters d_g, k_e, d_e for all joints. These unknown parameters are collected in the vector θ.

B. Frequency domain identification algorithm

A frequency-domain method is used for finding θ, as proposed in [10]. The method is based on the assumption that the excitation signal is a small perturbation around a robot configuration, allowing linearization of (1). The parameters $\hat{\theta}$ are obtained by minimizing the weighted log-error between the FRFs $\hat{G}^{(i)}(\omega)$, estimated from measurements (see Section III), and the parametric FRFs $G^{(i)}(\omega,\theta)$ of the linearized gray-box model (1):

$$\hat{\theta} = \arg\min_{\theta} \sum_{i\in Q_c}\sum_{l=1}^{N}\left[\mathcal{E}^{(i)}(\omega_l,\theta)\right]^{\mathrm{H}} W^{(i)}(\omega_l)\,\mathcal{E}^{(i)}(\omega_l,\theta)$$
$$\mathcal{E}^{(i)}(\omega_l,\theta) = \log\mathrm{vec}(\hat{G}^{(i)}(\omega_l)) - \log\mathrm{vec}(G^{(i)}(\omega_l,\theta)) \quad (2)$$

where N is the number of frequencies and Q_c a set of robot configurations. The logarithm of complex numbers is defined as $\log(X) = \log|X| + j\arg(X)$, where, e.g., $X = \mathrm{vec}(\hat{G}^{(i)}(\omega_l))$. $W^{(i)}(\omega)$ is a weighting matrix. The weights reflect both the uncertainty in $\hat{G}$, as well as the user choice of which FRF elements and frequency ranges are considered as most important to describe with the model [11]. Here, we choose to weight the diagonal elements of the FRFs and the frequency range around the first (anti)resonance highest, since these are most important for characterizing the system and, in particular, its stiffness parameters. The log-criterion is used because of the large dynamic range of the highly resonant robot system and because of its robustness w.r.t. outliers in the data [12]. The problem (2) is solved using MATLAB and *fminunc*. Since the objective function is not convex, reasonable initial values are needed, which can, e.g., be found from catalog data of the joint components and Finite Element Analysis as suggested in [13]. Furthermore, the problem is solved for a number of random perturbations around the initial guess. The linearization $G^{(i)}(\omega,\theta)$ is obtained from first order Taylor series expansion of (1). The linearization points i are chosen by the experiment design approach as in [14].

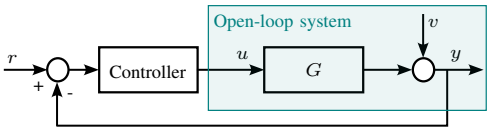

Fig. 2. Closed-loop system.

III. Classical methods for FRF estimation

Consider the setting in Figure 2, where u is the plant input (dimension n_u) and y is the measured output (dimension n_y), corrupted by measurement noise v. The goal is to obtain a nonparametric estimate of the system's frequency function G, as well as the noise covariance matrix $C_v = \mathrm{Cov}(v)$. The closed-loop setup is necessary for manipulator identification, since the system is nonlinear with gravity acting as a position-dependent disturbance on the input torque. Without feedback control active, the robot arm would drift away from the chosen configuration, making the linearization invalid and also introducing a risk for collision. The controller input is the difference between the reference signal r and the output y. The discrete Fourier transforms (DFTs) of the input and output signal are denoted as $U(\omega_k)$ and $Y(\omega_k)$, respectively, with the frequencies $\omega_k = k\frac{2\pi}{NT_s},\ k = 1, 2, \ldots, N$, where N is the total number of samples and T_s the sampling period. The DFTs of input and output are related as

$$Y(\omega_k) = G(e^{j\omega_k T_s})U(\omega_k) + V(\omega_k) \tag{3}$$

where $G(e^{j\omega_k T_s})$ is the system's $n_y \times n_u$ transfer function and $V(\omega_k)$ the noise DFT. In the following, the complex variable $\Omega_k = e^{j\omega_k T_s}$ is used.

Using classical nonparametric techniques for obtaining an estimate of $G(\Omega_k)$, $n_e \geq n_u$ experiments are needed, since (3) contains $n_y \cdot n_u$ unknown transfer functions. The data vectors from n_e experiments are collected into matrices (bold-face) where each column corresponds to one experiment. In the noise-free case, Eq. (3) becomes

$$\mathbf{Y}(\omega_k) = G(\Omega_k)\mathbf{U}(\omega_k) \tag{4}$$

where $\mathbf{Y}(\omega_k)$ and $\mathbf{U}(\omega_k)$ are $n_y \times n_e$ and $n_u \times n_e$. The solvability of (4) depends on the condition number of $\mathbf{U}$. One possible choice in this context is to use orthogonal random phase multisine signals for excitation as suggested in [15]. Different methods have been proposed for obtaining an estimate $\hat{G}(\Omega_k)$, e.g. the H1-estimator [16]:

$$\hat{G}^{\mathrm{H1}}(\Omega_k) = \mathbf{Y}(\omega_k)\mathbf{U}^{\mathrm{H}}(\omega_k)\left[\mathbf{U}(\omega_k)\mathbf{U}^{\mathrm{H}}(\omega_k)\right]^{-1} \tag{5}$$

where $(\cdot)^{\mathrm{H}}$ denotes the conjugate transpose.

For improving the quality of the estimate, we collect more data and assume that $n_e = M\,n_u$ experiments are done. Then, the DFT matrices can be partitioned into M blocks as

$$\mathbf{X}(\omega_k) = \left[\mathbf{X}^{[1]}(\omega_k) \ldots \mathbf{X}^{[M]}(\omega_k)\right] \tag{6}$$

where $\mathbf{X}$ stands for any of the signals $\mathbf{U}$, $\mathbf{Y}$ or $\mathbf{R}$. See Figure 3 for a visualization of the matrix structuring. The frequency argument ω_k will be omitted in the following. Then, the H1-estimator becomes

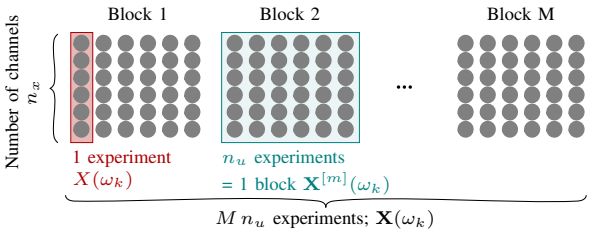

Fig. 3. Visualization of the data structuring for classical methods for FRF estimation.

$$\hat{G}^{\mathrm{H1}} = \left[\frac{1}{M}\sum_{m=1}^{M}\mathbf{Y}^{[m]}\mathbf{U}^{[m]\mathrm{H}}\right]\left[\frac{1}{M}\sum_{m=1}^{M}\mathbf{U}^{[m]}\mathbf{U}^{[m]\mathrm{H}}\right]^{-1} \tag{7}$$

Another method is the arithmetic mean estimator [17], given by $\hat{G}^{\mathrm{ARI}} = \frac{1}{M}\sum_{m=1}^{M}\hat{G}^{[m]}$, where $\hat{G}^{[m]} = \mathbf{Y}^{[m]}\left[\mathbf{U}^{[m]}\right]^{-1}$. The averaging can be generalized to nonlinear techniques, as in [17]. For a robotic system, and assuming $n_u = n_y$, the logarithmic technique has shown to give best results [2], estimating the FRF by

$$\hat{G}^{\mathrm{LOG}} = P^{-1}\exp\left(\frac{1}{M}\sum_{m=1}^{M}\log\left(P\,\hat{G}^{[m]}\right)\right) \tag{8}$$

where the matrix P is used to avoid phase wrapping problems when averaging the phase. It is chosen as

$$P = V^{[1]}\mathrm{diag}\left\{e^{-j\arg\lambda_l^{[1]}}\right\}_{l=1}^{n}[V^{[1]}]^{-1} \tag{9}$$

with the eigenvalue decomposition $\hat{G}^{[1]} = V^{[1]}\Lambda^{[1]}[V^{[1]}]^{-1}$, $\Lambda^{[1]} = \mathrm{diag}\left\{\lambda_l^{[1]}\right\}_{l=1}^{n}$. The log- and exp-functions are matrix functions $f(A), A \in \mathbb{C}^{n\times n}$, using the eigenvalue decomposition $f(A) = Vf(\Lambda)V^{-1} = V\mathrm{diag}\left\{f(\lambda_l)\right\}_{l=1}^{n}V^{-1}$, see [17].

Now, the closed-loop system of Figure 2 is considered and we assume that the reference signal r is available. Then, a joint input-output (JIO) approach can be applied:

$$\hat{G}^{\mathrm{JIO}} = \left[\frac{1}{M}\sum_{m=1}^{M}\mathbf{Y}^{[m]}\mathbf{R}^{[m]\mathrm{H}}\right]\left[\frac{1}{M}\sum_{m=1}^{M}\mathbf{U}^{[m]}\mathbf{R}^{[m]\mathrm{H}}\right]^{-1} \tag{10}$$

Since the JIO estimator is consistent and asymptotically unbiased, it will perform best as the number of measured data blocks M increases. This is also concluded in [18], where different averaging techniques are compared in a simulation study with a linear robot model. Compared to that, the experimental results in [2] show that (10) does not perform that well mainly due to large errors at low frequencies. Since it is based on the H1 estimator, Eq. (10) gives comparable estimates as (7), especially if only few experiments are considered, see Table I.

Here, the uncertainty of the averaged estimates (7), (8) and (10) is the sample variance over the M realizations (blocks):

$$\sigma^2_{\hat{G}} = \frac{1}{M(M-1)}\sum_{m=1}^{M}\left(\hat{G}^{[m]} - \hat{G}\right)\left(\hat{G}^{[m]} - \hat{G}\right)^{\mathrm{H}}$$

See [12, Chap. 4.3] for details.

IV. Local rational methods (LRM) for FRF estimation

The key idea of LRM is to assume that $G(\Omega_k)$ is a smooth function of frequency and that it can be approximated locally around a central frequency by a complex polynomial [3], [4]. Assuming a high signal-to-noise ratio, the open loop system indicated in Figure 2 is considered first. The closed-loop problem will be considered in Section IV-C. Assuming local parametric functions and using multiple data points within the window make it possible to obtain an estimate of $G(\Omega_k)$ with just one experiment, while classic non-parametric methods require data from $n_e \geq n_u$ experiments because only data points of one frequency are used at a time.

A. MISO parametrization

To begin with, every row $i = 1, \ldots, n_y$ of G is estimated separately by considering all n_u inputs $U = [U_1, \ldots, U_{n_u}]^T$ and one output Y_i at a time (MISO). Then, Eq. (3) at DFT line $\omega_{k+\tilde{r}}$ can be approximated with

$$Y_i(\omega_{k+\tilde{r}}) = G_i(\Omega_{k+\tilde{r}})U(\omega_{k+\tilde{r}}) + V_i(\omega_{k+\tilde{r}}) \tag{11}$$

where $G_i(\Omega_{k+\tilde{r}}) = [G_{i1}(\Omega_{k+\tilde{r}}), \ldots, G_{in_u}(\Omega_{k+\tilde{r}})]$ with

$$G_{ij}(\Omega_{k+\tilde{r}}) \;=\; G_{ij}(\Omega_k) + \sum_{s=1}^{R} g_{s,ij}(\omega_k)\tilde{r}^s \tag{12}$$

for $j = 1, \ldots, n_u$. Here, V_i denotes both the original noise component and the approximation error. $G(\Omega_k)$ is approximated with polynomials of order R in a sliding window of width $w = 2b + 1$, which is centered around a central frequency ω_k. $\tilde{r}$ is a component in r, where $r = [-b, \ldots, -1, 0, 1, \ldots, b]^T$, except near the frequency borders. Now, we consider rational functions as local approximations and Eq. (11) is modified to

$$Y_i(\omega_{k+\tilde{r}}) = \frac{G_i(\Omega_{k+\tilde{r}})}{D_i(\omega_{k+\tilde{r}})}U(\omega_{k+\tilde{r}}) + V_i(\omega_{k+\tilde{r}}) \tag{13}$$

The polynomial D_i is mainly added to reduce the approximation errors around anti-/resonances and is defined as

$$D_i(\omega_{k+\tilde{r}}) \;=\; 1 + \sum_{s=1}^{R} d_{s,i}(\omega_k)\tilde{r}^s\,, \tag{14}$$

see Parametrization 2 in [8]. Multiplying (13) with D_i gives

$$\begin{aligned} Y_i(\omega_{k+\tilde{r}}) = &\left(G_i(\Omega_k) + \sum_{s=1}^{R} g_{s,i}(\omega_k)\tilde{r}^s\right)U(\omega_{k+\tilde{r}}) \\ &- \left(\sum_{s=1}^{R} d_{s,i}(\omega_k)\tilde{r}^s\right)Y_i(\omega_{k+\tilde{r}}) + V_i(\omega_{k+\tilde{r}})D_i(\omega_{k+\tilde{r}}) \end{aligned}$$

Collecting the data from w frequency lines within a window, Eq. (13) can be re-written as

$$Y_{w,i} = K_{w,i}\Theta_i(\omega_k) + \tilde{V}_{w,i} \tag{15}$$

where $\tilde{V}_{w,i}$ is the noise term scaled with $D_{w,i}$. $Y_{w,i}$, $D_{w,i}$ and $\tilde{V}_{w,i}$ are $w \times 1$ complex vectors. The complex vector $\Theta_i \in \mathbb{C}^{[(R+1)n_u+R]\times 1}$ contains the unknown (local) parameters

$$\begin{aligned} \Theta_i(\omega_k) = &[G_{i1}, g_{1,i1}, \ldots, g_{R,i1}, \ldots, G_{i\,n_u}, \\ &g_{1,i\,n_u}, \ldots, g_{R,i\,n_u}, d_{1,i}, \ldots, d_{R,i}]^T \end{aligned} \tag{16}$$

The matrix $K_{w,i} \in \mathbb{C}^{w\times[(R+1)n_u+R]}$ contains the input data $U_w \in \mathbb{C}^{w\times n_u}$ within the window:

$$K_{w,i} = \left[[r^0\, r^1 \ldots r^R] \otimes U_w \;,\; -[r \ldots r^R] \otimes Y_{w,i}\right] \tag{17}$$

where $\otimes$ means that, e.g., each column of the $w \times (R+1)$-matrix $[r^0\, r^1 \ldots r^R]$ is multiplied with each column of U_w. All products are taken element-wise. The window width must be $w \geq w_{min} = (R+1)n_u + R$ in order to estimate all parameters Θ_i. (15) is linear in the parameters, but overdetermined if $w > w_{min}$. It can be solved using least squares as

$$\hat{\Theta}_i(\omega_k) = (K_{w,i}^{\mathrm{H}}K_{w,i})^{-1}K_{w,i}^{\mathrm{H}}Y_{w,i} \tag{18}$$

This is referred to as Local Levy method in [7]. It is noted, but not further considered in the scope of this paper, that the linearization of the output error yields a biased estimate [12, p. 301 f.]. Note also that a transient term is not estimated, since we will use periodic excitation and cut the data. The residual of the least-squares fit (18) and an estimate of the noise covariance are given by

$$\hat{V}_{w,i} = Y_{w,i} - K_{w,i}\hat{\Theta}_i(\omega_k) \tag{19}$$

$$\hat{C}_{V,i}(\omega_k) = \frac{1}{q}\hat{V}_{w,i}^{\mathrm{H}}\hat{V}_{w,i} \tag{20}$$

where $q = w - \mathrm{rank}(K)$, see [4].

Increasing w, which signifies the inclusion of a greater number of frequencies within the frequency window, leads to a reduction in the variance of the parameter estimate. This reduction is due to the noise being averaged across a more extensive array of data points. Conversely, expanding the frequency window increases the interpolation error, which arises from the variation of the transfer function over the interval in question. In practice, the LPM is mostly used with polynomials of degree two, i.e. $R = 2$ [6].

B. MIMO parametrization

Since the robot operates in closed loop, all outputs affect the system through feedback, and we therefore consider all outputs Y_i simultaneously in the following. Then, $Y = [Y_1, \ldots, Y_{n_y}]$, and D_w becomes a $n_y \times n_y$-matrix of polynomials (full MFD parametrization, see Parametrization 3 in [8]). Then, analogous to (15),

$$Y_w = K_w\Theta(\omega_k) + \tilde{V}_w \tag{21}$$

where Y_w and $\tilde{V}_w$ are $w \times n_y$ matrices and $\Theta(\omega_k) = [\Theta_1(\omega_k), \ldots, \Theta_{n_y}(\omega_k)]$ is the $(R+1)n_u + R\,n_y \times n_y$ matrix of unknown parameters. For $i = 1 \ldots n_y$,

$$\begin{aligned} \Theta_i(\omega_k) = [&G_{i1},\, g_{1,i1}, \ldots, g_{R,i1}, \ldots, G_{i\,n_u},\, g_{1,i\,n_u}, \ldots, \\ &g_{R,i\,n_u},\, d_{1,i1}, \ldots, d_{R,i1}, \ldots, d_{1,i\,n_y}, \ldots, d_{R,i\,n_y}]^T \end{aligned} \tag{22}$$

Now, $w_{min} = (R+1)n_u + R\,n_y$, and $K_w \in \mathbb{C}^{w\times[(R+1)n_u+R\,n_y]}$ is:

$$K_w = \left[[r^0\, r^1 \dots r^R] \otimes U_w \;,\; -[r \dots r^R] \otimes Y_w\right] \tag{23}$$

This approach has the advantage that the cross-influence of the different outputs is taken into account through the parameters of the polynomials in the matrix D.

Analogous as in (19) and (20), the uncertainty of the FRF estimate is derived from the residuals as

$$\hat{\hat{V}}_w(\omega_k) = Y_w - K_w\hat{\Theta}(\omega_k) \tag{24}$$

$$\hat{C}_{\hat{V}_w}(\omega_k) = \frac{1}{q}\hat{\hat{V}}_w^{\,\mathrm{H}}(\omega_k)\hat{\hat{V}}_w(\omega_k)\,. \tag{25}$$

C. Joint input-output approach

Assuming the closed-loop system of Figure 2, and that the reference signal r is available, the following joint input-output (JIO) approach can be applied [19], [20, p. 438]: First, the FRFs $\hat{G}_{ru}$ and $\hat{G}_{ry}$ from the reference r to the input u, and from the reference r to the output y are estimated using LRM. Second, the FRF from u to y is computed as the ratio $\hat{G}_{ry}/\hat{G}_{ru}$. We will call this variant JIO-LRM in the following.

D. Involving multiple experiments

For improving the LRM estimate, multiple experiments can be done and logarithmic averaging can be applied. Then, $\hat{G}^{[m]}$ in (8) is replaced by the LRM estimate and M is replaced by n_e, since LRM delivers an estimate for each single experiment.

V. Results

A. Excitation design and measurement signals

An orthogonal random phase multi-sine signal is chosen for excitation, containing 336 log-spaced odd frequencies in the range 4 - 80 Hz. All motors are excited simultaneously with a speed reference. For the purpose of linearization, the robot must be kept in a quasi-static position close to the chosen configuration, but in order to reduce the effect of static friction, zero velocity should be avoided. Thus, we add a low-frequent single sine with sufficiently large amplitude to the reference [21]. Using the available sensors, motor currents and angular positions are logged at 2 kHz. The motor torques (u) are computed with a simple linear relationship between motor current and torque (The motor dynamics are much faster than the dynamics of the manipulator arm.). The angular positions are numerically differentiated to become motor accelerations (y). The period time for one experiment is 28 s. The FRFs are estimated in several linearization points, i.e. several random robot configurations distributed in the work-space.

Both real experiments and simulations are done. Figure 4 illustrates the framework. In simulation, a robot model (1) with parameters θ_0 is excited around configurations i and its FRFs $G^{(i)}(\omega, \theta_0)$ are computed. The robot plant is simulated with a controller, consisting of a basic P-type position controller with an inner velocity loop of PI-type. White noise

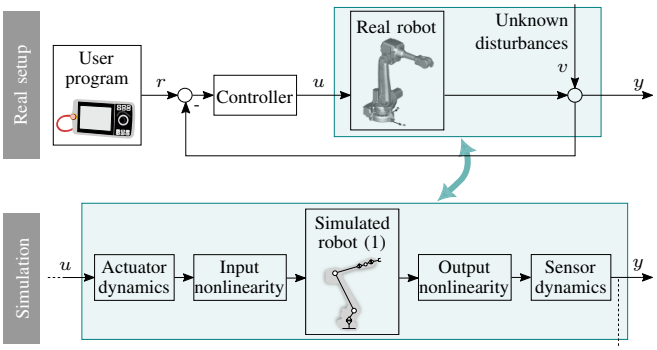

Fig. 4. Framework for real experiments and simulation.

and deterministic position dependent disturbances are added to the simulated motor position. Moreover, deterministic position dependent disturbances are added to the motor torque for simulating motor torque ripple. All deterministic disturbances are periodic in the motor position and therefore described as a sum of sinusoids. All disturbances are tuned such that the simulation generates data that is very similar to the real data.

B. FRF estimation using real data

FRFs are estimated using the real system as illustrated in the upper part of Figure 4. The logarithmic FRF estimate (8) with $M = 4$ blocks of data serves as reference, i.e. data from $n_e = Mn_u = 24$ experiments is used. Estimates involving fewer experiments are compared. $\hat{G}$ is derived with the (MISO-, MIMO-, JIO-) LRM and H1 methods using only $n_e = 6$ experiments. Note that the H1 and LOG estimator are identical if $M = 1$, i.e. $n_e = 6$. The MIMO parametrization of Section IV-B is used for JIO-LRM, and logarithmic averaging is applied for merging the 6 LRM estimates. Furthermore, an estimate using JIO-LRM that is derived from only one experiment is included. For the LRM, second order polynomials are used, i.e. $R = 2$, and a window slightly wider than w_{min} is chosen ($w = w_{min} + 2 = 20$) for getting a smoother estimate.

Figure 5 shows the FRF estimates of an exemplary robot configuration obtained from real data. See also Figure 6, which shows an enlargement of $G_{3,3}$ (upper part) and the absolute error relative to LOG_{24} (lower part). The H1 method (7) gives a noisy estimate if only 6 experiments are used ($\mathrm{H1}_6$), which is the minimum for this method. Collecting more data by exciting the motors with different realizations of the reference signal, logarithmic averaging can be applied. Figure 5 shows the LOG estimate (8) with $M = 4$ blocks data (LOG_{24}). Note that no windowing technique is applied, i.e. the FRF is computed at every excited frequency separately and averaged with the estimate from other experiments, which are independent realizations of the input signal. Assuming LOG_{24} as *the truth* and comparing the FRFs estimated with LRM, the most obvious observation is that the damping of the resonances is over-estimated using $\mathrm{MIMO\text{-}LRM}_6$. Compared to that, the anti-resonances can be estimated more accurately. The fact that

the resonance peaks are hard to estimate with LRM has been observed in [7], and has been explained by overemphasis of the noise at the borders of the local frequency band. The JIO-LRM estimate is much better around the resonance peaks, indicating that using the reference signals is crucial for local methods, while it seems to be less important for classical averaging techniques. Even JIO-LRM$_1$, which is obtained from only one experiment, succeeds in estimating the frequency location of the resonances. The damping is much lower compared to the LOG-estimate and the estimate for low frequencies yields a large error for the robot's wrist axes (G_{44} to G_{66}).

C. Validation using simulated data

For further validation of the different FRF estimates, a nonlinear robot model with parameters θ_0 is simulated in closed loop with added disturbances, see lower part of Figure 4. A weighted amplitude bias is computed as

$$\frac{1}{N\,Q}\sum_{i=1}^{Q}\sum_{l=1}^{N}\left\|W^{(i)^T}(\omega_l)\left[|G^{(i)}(\omega_l,\theta_0)|-|\hat{G}^{(i)}(\omega_l)|\right]\right\|_2 \tag{26}$$

where Q is the number of robot configurations and W the weighting matrix from (2). $|\cdot|$ denotes the elementwise absolute value and $\|\cdot\|_2$ the matrix 2-norm. There will be a bias (26) due to, e.g., deficiencies in the data, nonlinearities and the controller impact. Table I shows the bias for $Q = 49$ random configurations. The MIMO-LRM estimate gives a smaller bias compared to MISO-LRM, if $n_e > 1$, demonstrating that the choice of parametrization is crucial for the method. Since excitation of one axis affects all other axes, the outputs cannot be treated independently, which needs to be considered in the polynomials of D in (21). Using LRM, the JIO-approach leads to a significant bias reduction. Compared to that, the JIO estimate (10) yields only a small improvement compared to LOG (8). In order to achieve short measurement times, minimal estimation data shall be used, i.e. the last entries in each column of Table I are compared: JIO-LRM with $n_e = 1$ gives the lowest FRF amplitude bias. In particular, it is lower than the bias of averaged estimates with 1 block of experiments ($n_e = 6$).

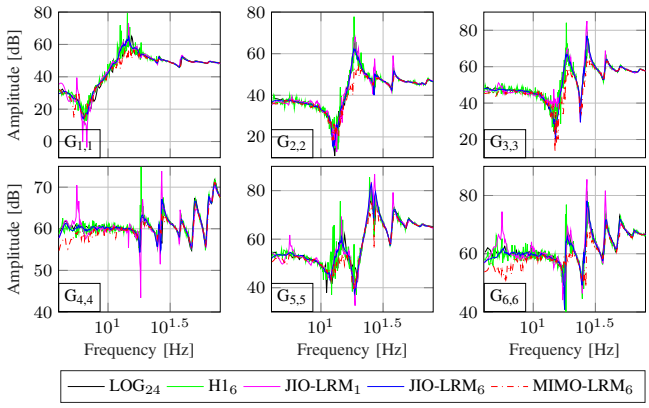

Fig. 5. Diagonal elements of $\hat{G}$ estimated from n_e experiments (n_e indicated as indices in the legend).

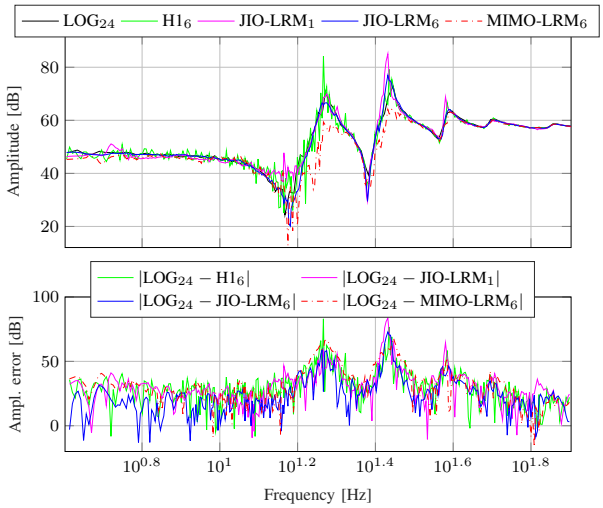

Fig. 6. Enlargement of $G_{3,3}$ from Figure 5 (upper figure) and corresponding absolute error relative to LOG$_{24}$ (lower figure).

VI. Parametric Model Identification

It was shown in the previous section that additional experiments, i.e. $n_e > 1$, improve the FRF accuracy. Aiming to estimate the parameters of the gray-box model (1) with data collected in minimal experiment time, a trade-off needs to be made between experiment time and FRF quality. In this section, the stiffness parameters of the model (1) are estimated using the algorithm in Section II-B. The different nonparametric FRF estimates from Section V-B are used for estimation and the resulting model parameters θ are compared. The aim is to find a FRF estimation method suitable in the context of parametric gray-box identification.

In order to measure the quality of the derived parametric models, data is obtained from simulation where the true model with parameters θ_0 is known. The JIO-LRM and the LOG[1] methods are compared in Table II w.r.t. their average bias $\bar{B}_\theta = \frac{1}{p}\sum_{s=1}^{p}\frac{|\theta_{0,s}-\hat{\theta}_s|}{\theta_{0,s}}$, $p = \dim(\theta)$. The estimation data was generated in 7 robot configurations, found by using the experiment design proposed in [14]. Either 24, 6 or 1

[1]Since JIO (Eq. (10)) gives a similar FRF bias (Table I) but requires the recording of the reference signals, LOG (Eq. (8)) is preferred.

TABLE I

Bias of FRF amplitude (26); Avg. of 49 robot configurations.

n_e per configuration	LOG (Eq. (8))	JIO (Eq. (10))	LRM, MISO	LRM, MIMO	LRM, JIO
24 ($M = 4$)	135.55	134.72	248.65	240.40	125.22
6 ($M = 1$)	162.14	162.14	257.71	249.89	136.20
1	–	–	238.89	238.90	147.27

TABLE II

MEAN BIAS $\bar{B}_\theta = \frac{1}{p}\sum_{s=1}^{p} \frac{|\theta_{0,s} - \hat{\theta}_s|}{\theta_{0,s}}$ OF THE MODEL PARAMETERS; ESTIMATION DATA FROM n_e EXPERIMENTS IN 7 CONFIGURATIONS.

	$n_e = 1$	$n_e = 6$		$n_e = 24$	
Method	JIO-LRM	LOG (8)	JIO-LRM	LOG (8)	JIO-LRM
$\bar{B}_\theta$	19.1 %	10.0 %	9.1 %	7.9 %	4.8 %

experiments were simulated in each configuration. A bias occurs between θ_0 and $\hat{\theta}$ due to unmodeled nonlinearities such as nonlinear transmission stiffness, and closed-loop effects. The bias of most parameters in θ is less than 3 %, but two parameters have a bias in the range of 20-50 %.

The average parameter bias is lowest if data from 24 experiments is used together with the JIO-LRM method. In general, the JIO-LRM outperforms the traditional LOG-avg method, if the same experiment time is assumed. Note that JIO-LRM requires the reference signals to be recorded. Even though the FRF amplitude bias for JIO-LRM with $n_e = 1$ is lower than the bias of LOG with $n_e = 6$ (Table I), the parametric model which is estimated from the latter is more accurate in terms of $\bar{B}_\theta$. It should also be noted that the results in Table II depend on the chosen excitation signal, as well as the robot configurations selected for the experiments. Depending on the intended use of the parametric model, a larger bias in some components of θ might be acceptable. From a practical point of view, a trade-off needs to be made between parameter accuracy and experiment time.

VII. CONCLUSIONS

In order to keep the experiment time as low as possible, the data-efficient LRM method was applied for estimating nonparametric FRFs of a 6-axes robot. The resulting FRFs were compared to classical, purely nonparametric, estimates obtained from multiple experiments. Furthermore logarithmic averaging of multiple FRF estimates was compared. The presented results of an experimental study showed that a MIMO parametrization in LRM gives a more accurate FRF estimate compared to a MISO parametrization. Furthermore, the benefit of a JIO approach combined with LRM was shown, as well as the possible improvement by additional experiments and logarithmic averaging. The presented results suggest that the JIO-LRM method combined with LOG-averaging gives the most accurate FRF estimate among the compared methods, assuming the same measurement time. Since the LRM estimate with minimum data, i.e. one experiment, gives only poor identification results for the parametric robot model, it is concluded that a trade-off needs to be made between experiment time and identification accuracy. Further research on local parameterizations as well as the effects of nonlinearities in the system is recommended in order to improve the LRM estimate and in order to reduce the parameter bias of the gray-box robot model.

VIII. ACKNOWLEDGMENTS

This work was sponsored by the Vinnova competence center LINK-SIC.

REFERENCES

[1] E. Wernholt, "Multivariable Frequency-Domain Identification of Industrial Robots," *0345-7524*, no. 1138, 2007.

[2] E. Wernholt and S. Moberg, "Experimental comparison of methods for multivariable frequency response function estimation," *IFAC Proceedings Volumes (IFAC-PapersOnline)*, vol. 17, no. 1 PART 1, 2008.

[3] T. McKelvey and G. Guérin, "Non-parametric frequency response estimation using a local rational model," *IFAC Proceedings Volumes*, vol. 45, no. 16, pp. 49–54, 2012.

[4] R. Pintelon, J. Schoukens, G. Vandersteen, and K. Barbé, "Estimation of nonparametric noise and FRF models for multivariable systems—Part I: Theory," *Mechanical Systems and Signal Processing*, vol. 24, no. 3, pp. 573–595, 2010.

[5] ——, "Estimation of nonparametric noise and FRF models for multivariable systems—Part II: Extensions, applications," *Mechanical Systems and Signal Processing*, vol. 24, no. 3, pp. 596–616, 2010.

[6] M. Gevers, R. Pintelon, and J. Schoukens, "The Local Polynomial Method for nonparametric system identification: Improvements and experimentation," in *IEEE Conference on Decision and Control and European Control Conference*. IEEE, 2011, pp. 4302–4307.

[7] R. Pintelon, D. Peumans, G. Vandersteen, and J. Lataire, "Frequency Response Function Measurements via Local Rational Modeling, Revisited," *IEEE Transactions on Instrumentation and Measurement*, vol. 70, pp. 1–16, 2021.

[8] R. Voorhoeve, A. van der Maas, and T. Oomen, "Non-parametric identification of multivariable systems: A local rational modeling approach with application to a vibration isolation benchmark," *Mechanical Systems and Signal Processing*, vol. 105, pp. 129–152, 2018.

[9] J. Öhr, S. Moberg, E. Wernholt, S. Hanssen, J. Pettersson, S. Persson, and S. Sander-Tavallaey, "Identification of flexibility parameters of 6-axis industrial manipulator models," *Proceedings of ISMA2006: International Conference on Noise and Vibration Engineering*, vol. 6, 2006.

[10] E. Wernholt and S. Moberg, "Frequency-Domain Gray-Box Identification of Industrial Robots," *IFAC Proceedings Volumes*, vol. 41, no. 2, pp. 15 372–15 380, 2008.

[11] S. Moberg, E. Wernholt, S. Hanssen, and T. Brogårdh, "Modeling and Parameter Estimation of Robot Manipulators Using Extended Flexible Joint Models," *Journal of Dynamic Systems, Measurement, and Control*, vol. 136, no. 3, 2014.

[12] R. Pintelon and J. Schoukens, *System identification: A frequency domain approach*, 2nd ed. Hoboken, N.J.: John Wiley & Sons Inc, 2012.

[13] S. A. Zimmermann, T. F. C. Berninger, J. Derkx, and D. J. Rixen, "Dynamic modeling of robotic manipulators for accuracy evaluation," in *2020 IEEE International Conference on Robotics and Automation (ICRA)*. Piscataway, NJ: IEEE, 2020, pp. 8144–8150.

[14] S. A. Zimmermann, M. Enqvist, S. Gunnarsson, S. Moberg, and M. Norrlöf, "Experimental evaluation of a method for improving experiment design in robot identification," in *2023 IEEE International Conference on Robotics and Automation (ICRA)*. IEEE, 2023, pp. 11 432–11 438.

[15] T. Dobrowiecki and J. Schoukens, "Measuring a linear approximation to weakly nonlinear MIMO systems," *Automatica*, vol. 43, no. 10, pp. 1737–1751, 2007.

[16] P. Guillaume, R. Pintelon, and J. Schoukens, "Accurate Estimation of Multivariable Frequency Response Functions," *IFAC Proceedings Volumes*, vol. 29, no. 1, pp. 4351–4356, 1996.

[17] P. Guillaume, "Frequency response measurements of multivariable systems using nonlinear averaging techniques," *IEEE Transactions on Instrumentation and Measurement*, vol. 47, no. 3, pp. 796–800, 1998.

[18] E. Wernholt and S. Gunnarsson, "Analysis of methods for multivariable frequency response function estimation in closed loop," in *46th IEEE Conference on Decision and Control*. Piscataway, N.J.: Institute of Electrical and Electronics Engineers, 2007, pp. 4881–4888.

[19] P. E. Wellstead, "Non-parametric methods of system identification," *Automatica*, vol. 17, no. 1, pp. 55–69, 1981.

[20] L. Ljung, *System identification: Theory for the user*, 2nd ed. Upper Saddle River, N.J.: Prentice Hall, 1999.

[21] E. Wernholt and S. Gunnarsson, "Estimation of Nonlinear Effects in Frequency Domain Identification of Industrial Robots," *IEEE Transactions on Instrumentation and Measurement*, vol. 57, no. 4, pp. 856–863, 2008.